

AUTOSTEREOSCOPIC VISUALIZATION AND MEASUREMENT: PRINCIPLES AND EVALUATION

Jie Shan, Chiung-Shiuan Fu, Bin Li, James Bethel, Jeffrey Kretsch*, Edward Mikhail

Geomatics Engineering, School of Civil Engineering, Purdue University
550 Stadium Mall Drive, West Lafayette, IN 47907-2051, USA, jshan@ecn.purdue.edu

Commission V, WG V/6

KEY WORDS: Visualization, Stereo, Vision, Measurement, Computer graphics, Photogrammetry

ABSTRACT:

Autostereoscope is a technology that allows for a viewer to obtain stereoscopic effect without wearing glasses. This may potentially be used as a replacement or alternative to the current goggle-based stereoscopic technologies used in visualization and mapping practice. This paper studies the principles of popular autostereoscopic technologies, fundamental issues in using this technology for visualization, photogrammetry, and the performance of autostereoscopic photogrammetric measurement. In particular, the autostereoscopic effect is studied in terms of viewing zone and perceived depth. As a fundamental step towards autostereoscopic photogrammetry, the imaging geometry of such displays is analytically presented. To evaluate the properties and performance of the autostereoscopic measurement, we conduct a series of experiments using a backlight autostereoscopic display. A stereo pair at a pixel size of 25 and 50 microns are used in the study. Three dozens of well defined and easily identified feature points are measured by seven operators using the developed autostereoscopic measurement toolkit Auto3D. The consistency of these measurement results is analyzed. In addition, they are also compared with the ones obtained from regular stereoscopic display. The work is a primary effort towards lighter and mobile image interpretation and measurement environment.

1. INTRODUCTION

Accurate and realistic 3D data collection and interpretation require stereoscopic observation. Although photogrammetry has been using stereo instruments for over a century, continuous development in stereo display industry provides many alternatives. In particular, the recent autostereoscopic technology has been brought into the attention of photogrammetrists and photogrammetry instrument vendors (Petrie, 2001). In contrast to the traditional photogrammetric technologies, autostereoscopic measurement is goggle-free (Okoshi 1980; Motoki et al 1995) or aid-free (Petrie, 2001), and can be used in mobile and field environment. This advantage contributes possible technical alternatives in photogrammetric practice and attracts emerging research on autostereoscopic mapping and interpretation system (Petrie, 2001).

However, the performance of this new technology needs to be thoroughly evaluated in terms of interpretation and mapping capabilities. In this paper, we study the measurement properties of the autostereoscopic display and conduct several photogrammetric tests to evaluate the performance of autostereoscopic measurement as a possible technical alternative for photogrammetric practice. A brief introduction to the principles of the autostereoscopic technology is first presented. We then quantitatively show the 3D autostereoscopic geometry, including the exact geometric shape of viewing zone, the movement boundary of operators for autostereoscopic measurement, and the perceived depth. The movement boundary is important for measurement because operators' 3D perceived depth varies according to the position of their eyes. To carry out autostereoscopic measurement and evaluate its performance, a photogrammetric toolkit Auto3D is developed based on the DTI autostereoscopic monitor. Design

considerations in the Auto3D development are discussed. Finally, we compare autostereoscopic measurement results with the ones obtained from common monoscopic and stereoscopic tools. Multiple operators are involved in the tests by measuring a number of carefully selected feature points. The results and discussion of the photogrammetric experiments are presented in this paper.

2. AUTOSTEREOSCOPIC PRINCIPLE

Here the term "autostereoscope" is to indicate that a viewer can perceive 3D information without viewing aids, such as goggles and spectacles. The most popular autostereoscopic technologies are parallax barrier (Okano et al, 1999; Sexton, 1992) and lenticular plate (Sexton 1992, Pastoor and Wöpking 1997). However, the general principle of an autostereoscopic system can be described by using the parallax barrier geometry (Okoshi, 1976; 1980). As shown in Figure 1, the parallax stereogram, an image that comprises interleaving stripes from the left and right images of a stereo pair, is placed in front of a barrier made of opaque material with periodic transparent vertical slits. Each fine transparent slit acts as a window to the corresponding image stripes. The stereogram and barrier are so arranged that the left eye and right eye of a viewer only perceive the corresponding left image and right image, respectively. Therefore, the barrier creates several 3D viewing zones to provide the binocular parallax according to the viewer's position. Similar to this general principle, the lenticular plate consists of an array of cylindrical lenticular lenses instead of parallax barrier (Hattori, 1991). Both lenticular and parallax barrier techniques support multiple viewing zones while the viewer moves the position.

* with the National Geospatial-Intelligence Agency

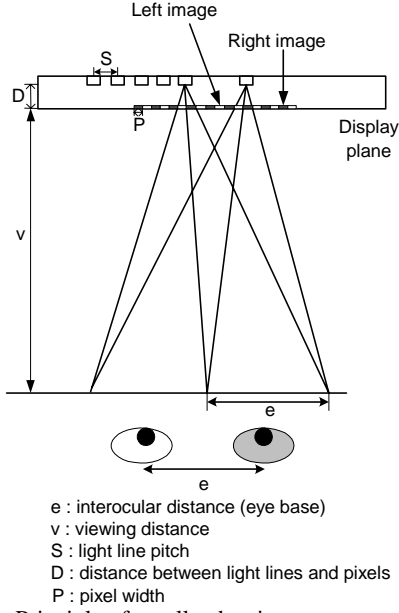


Figure 1. Principle of parallax barrier autostereoscope.

3. AUTOSTEREOSCOPIC EFFECT

3.1 3D Viewing Zone

The principle of the above autostereoscopic technology implies that a viewer can only acquire stereoscopic effect in certain locations and range, which is hereafter referred as viewing zones (Son et al, 2003). This will be studied geometrically as shown below.

The 3D geometry of viewing zones for a general autostereoscopic display panel is depicted in Figure 2, where the origin of the coordinate (x, y, z) is located at the central point of the monitor, W and H are respectively the width and height of the monitor. The lights emerging from both the left and right images cross each other and illustrate multiple viewing zones that are shaped to different volumetric diamond structures. The optimum viewing zones with horizontal parallax are located along the nominal viewing line parallel with x -axis and at the viewing distance v away from the display plane. For an autostereoscopic system, the value of v has been optimized according to the pitch of the barrier or the lenticular. In general, the number of the optimum viewing zones, N , is limited by W/e , where e is the eye base. Therefore, the n optimum viewing zones located left or right alternately from the center $(0,0,v)$ could be denoted by $n = \pm 1, \pm 2, \dots, \pm N/2$. Each diamond-type viewing zone can be regarded as the combination of two triangular pyramids which are referred as front pyramid and rear pyramid. For convenience, in Figure 3 we draw the projection of the viewing geometry on the xz -plane and show the projection of the pyramids as front triangle and rear triangle, respectively.

In Figure 3 the light from $(W/2, 0, 0)$ to $(0, 0, v)$ is denoted by R_0 and each light from $(W/2, 0, 0)$ to $(ne, 0, v)$ is denoted by R_n . Similarly the light from $(-W/2, 0, 0)$ to $(0, 0, v)$ is represented by L_0 and each light from $(-W/2, 0, 0)$ to $(ne, 0, v)$ is represented by L_n . Because the ideal width of the viewing zone under 2D projection is the average eye base, viewers can move their heads freely inside each viewing zone. Consequently, it is necessary to estimate the volume of each 3D diamond shape as

the movement boundary for operators implementing the photogrammetric practices.

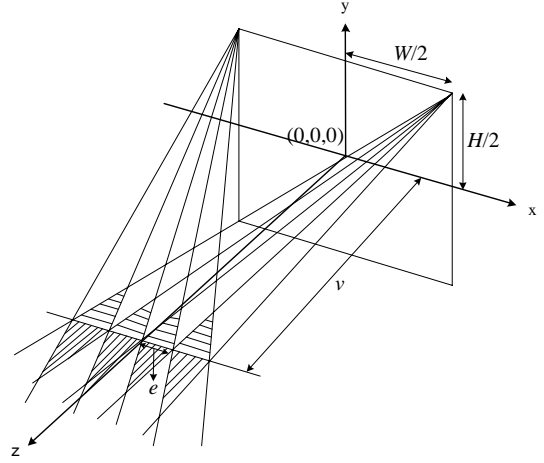


Figure 2. 3D viewing zones for an autostereoscopic display

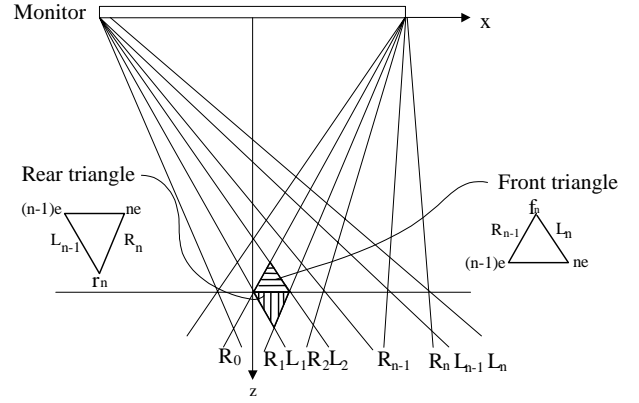


Figure 3. Projection of the viewing geometry on xz -plane with front triangle and rear triangle in viewing zone.

Based on the 3D coordinate system shown in Figure 2 and its xz -projection shown in Figure 3, we can address the range of viewing zone and the movement boundary for viewers. Let h_p represent the distance between the pixel and x -axis on xy -plane at $z=0$ and h_e denote the distance between operator's eyes and x -axis on xy -plane at $z=v$. For the front triangle, the coordinates of triangle points $(n-1)e$, ne and fn are defined by the following coordinate pairs

$$\begin{aligned}
 & ((n-1)e, h_e, v), \\
 & (ne, h_e, v), \\
 & \left(\frac{We(2n-1)}{2(W+e)}, \frac{Wh_e + eh_p}{W+e}, \frac{Wv}{W+e} \right). \quad (1)
 \end{aligned}$$

Based on this, we can calculate the volume of front pyramid as $WevH/(6W+6e)$ and the area of front triangle as $Wev/(2W+2e)$. Similarly, the coordinates of rear triangle points $(n-1)e$, ne and r_n are

$$\begin{aligned}
 & ((n-1)e, h_e, v), \\
 & (ne, h_e, v), \\
 & \left(\frac{We(2n-1)}{2(W-e)}, \frac{Wh_e - eh_p}{W-e}, \frac{Wv}{W-e} \right). \quad (2)
 \end{aligned}$$

The volume of rear triangular pyramid is $WevH/(6W-6e)$ and

the area of rear triangle is $Wev/(2W - 2e)$.

Equations (1) and (2) define the movement boundary for operators during autostereoscopic measurement. Within this boundary, operators can move their heads forward, backward, upward, and downward and still perceive correct 3D images. The free space in which the operators can move depends on the monitor size, the viewing distance and eye base. It is also shown that the front range f_n is slightly smaller than the rear range r_n . In our DTI monitor, the front range and rear range are respectively estimated as 10.8 and 14.2 cm from nominal viewing line, yielding totally 25 cm continuous range for a viewer to adjust his or her position in the direction perpendicular to the screen plane. This study also shows that the trapezoids of all viewing zones have the same volume.

For the DTI monitor in our study, the number of viewing zone is 7. A viewer can obtain stereo effect in seven locations by adjusting his or her position laterally. It should be noted that these are the locations that perfect stereo effect is ensured. In fact, a viewer can move his or her head outside the range defined by the monitor width. Therefore, there are practically more than 7 zones where viewers can receive stereo effect. However, since the viewing direction is not right perpendicular to the monitor in this situation, the magnitude of the light transmitted to the viewer's eyes is considerably reduced. As a result of this, the stereo view will become darker while the viewer positions are away from the screen center.

3.2 Perceived Depth

Human eyes are able to perceive depth to view 3D objects and distinguish the distance correctly (Jones et al, 2001). The perceived depth of an autostereoscopic mapping system determines the resolution for the object elevation to be measured. Hence the geometry of perceived depth should be discussed. The perceived depth is caused by horizontal parallax, which is the distance between corresponding points in two different images. When the correct stereo view is observed, the two optical axes intersect in front of the display plane. The image presented to the right eye of the observer appears to the left, and the left image presented to the left eye will appear to the right. The perceived depth appears in the front of display plane. The geometry is shown in Figure 4.

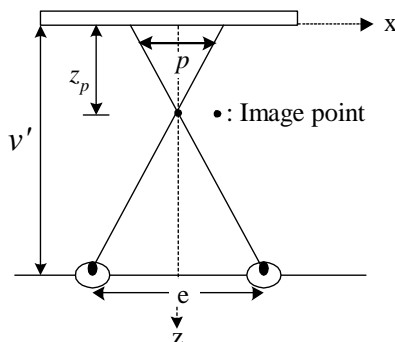


Figure 4. Perceived depth in front of the display plane.

In Figure 4, v' denotes the distance between display and viewer's eyes; p is represented the parallax of corresponding points on two images. The perceived depth z_p is the offset term ahead the display to the image point fused by viewer's

eyes. The geometry relation is given as $p/z_p = e/(v' - z_p)$. Thus the relationship between the perceived depth z_p and the viewing distance can be written as

$$z_p = \frac{pv'}{e + p} \quad (3)$$

If we treat e and p as constants, the perceived depth is linearly proportion to the viewing distance. From Eq. (3) when viewer's head moves toward to the display plane, the perceived depth becomes shorter; viewer's head moves away from the display plane, the perceived depth becomes longer from the display plane. The change of perceived depth inside the viewing zone is also linearly proportion to the change of viewing distance

$\Delta z_p = \frac{P}{e + p} \Delta v'$. According to the geometry of viewing zone, the limitation of viewer's head moving boundary inside the viewing zone is $\Delta v' = 2ev(W + e)/[W(W + 2e)]$ in xz -plane. Therefore, the maximum change of perceived depth inside the viewing zone is

$$\Delta z_p = \frac{P}{e + p} \{2ev(W + e)/[W(W + 2e)]\} \quad (4)$$

If the e and viewing distance v' are treated as constants, the differentiation of Eq. (3) with respect to the desired variable p directly yields

$$dz_p = \frac{v'e}{(e + p)^2} dp \quad (5)$$

Eq. (5) is the relationship between the perceived depth difference and the horizontal parallax difference. Assuming $e = 6.5 \text{ cm}$, $p = 1$ to 25 cm, we can plot Eq. (5) to Figure 5 for different viewing distances.

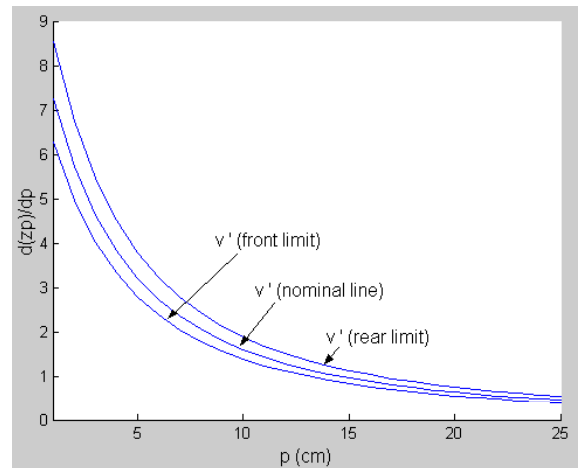


Figure 5. Ratio of perceived depth difference and parallax difference.

As is shown, the perceived depth difference is dependent on the parallax difference of the images. The relationship is not linear. In general, z_p is inversely proportional to the horizontal parallax; the perceived depth is directly proportional to the viewing distance. The perceived depth difference dz_p is amplified under autostereoscopic mode because the parallax p is small comparing to the view distance. This is a good property of autostereoscopic monitor. This means the horizontal parallax difference dp can be more apparently reflected in the change of perceived depth dz_p .

4. AUTO3D TOOLKIT

The display device used in this study is the 2018XL autostereoscopic monitor manufactured by DTI Inc., USA. It is 2D and 3D compatible and uses backlight technique to generate a sequence of light at certain frequency. Its maximum display resolution is 1280x1024 pixels. Unlike other popular autostereoscopic monitors, this monitor supports only two channels; therefore, the resolution is higher than other multi channel displays. A summary of the main specifications of the DTI monitor used in this study can be found in (Shan et al, 2004).

In order to evaluate the performance of autostereoscopic measurement, we developed a toolkit Auto3D based on the DTI autostereoscopic monitor. Auto3D is developed using Microsoft Visual C++ 6.0 with Multiple Document Interface/View frameworks. It can load, display and manipulate two images, conduct autostereoscopic measurement, label, and finally export the results. Figure 6 presents the main image measurement windows of Auto3D.

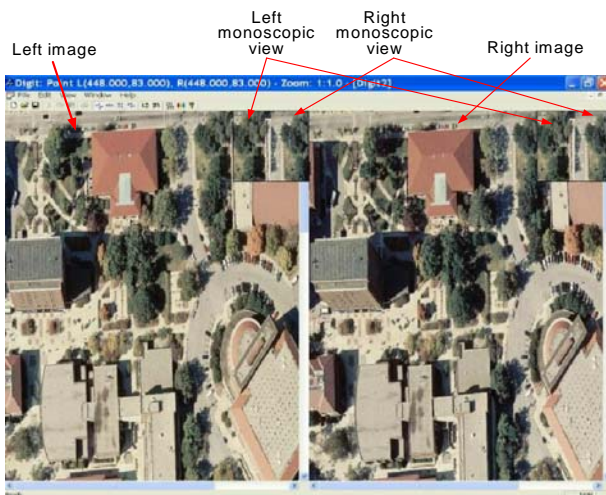


Figure 6. Auto3D interface (Purdue campus images)

The 3D viewing zones of this autostereoscopic monitor are created by parallax barriers. As discussed earlier, the principle of barrier-based system requires the two images of a stereo pair displayed being interleaved in columns. This indicates the horizontal resolution of the stereoscopic view is only half of the vertical resolution. Therefore, it is necessary to resample the two images properly to obtain both correct and sharp stereoscope. For this requirement, we duplicate the rows of the two original images for high quality application. Although this essentially doubles the image size for 3D display, as a trade-off the full resolution of the original images is retained. Moreover, the objective of image measurement is to obtain the image coordinates of feature points, such as corner point, line intersection, or T-junction, which should therefore be easily identified on the images. Consequently, Auto 3D is designed to handle two full-resolution images of a stereo pair.

The 3D measurement in Auto3D is based on dual floating marks. Unlike many other digital photogrammetric systems, these two floating marks need to be an ellipse with major axis in the vertical direction. In this way, the interleave process in DTI monitor will create one circular cursor under 3D mode. This dual design also applies to any graphic interface that is desired to be viewed as 2D. This property may essentially

double the work of software design and development (Shan et al, 2004).

For data collection, Auto3D can currently digitize point features on the images. Properties of labeled points can be changed, colored, stored into a data file, and later loaded for either adding new measurements or editing previously existent measurements. Furthermore, with two cursors on the left and right views, Auto3D's internal frames can simultaneously display two images and their corresponding two pairs of monoscopic views in one document as shown in Figure 6. Each pair of monoscopic views includes individual left and right images. To start measuring the coordinates of features points, move these two images toward or away from each other by rolling mouse wheel to adjust x-parallax until the feature points observed under the 3D condition have the best stereo perception. Checking the small monoscopic views, we can confirm that both cursors on the left and right images are located on the identical position of the feature point and obtain accurate height information.

5. TESTS AND EVALUATION

5.1 Tests data and equipments

Tests are designed to evaluate the performance of autostereoscopic measurement by comparing the results from different operators and from different equipments. To do so, a stereo pair at scale 1:4000 are scanned at a resolution of 33- μ m pixel size. Then, they are first epipolar normalized to remove possible y-parallax. The normalized images are resampled to two different resolutions, one at 25- μ m pixel size and the other at 50- μ m pixel size, which are used as the test images in our study. Two types of well-defined feature points are selected: 18 points on the ground and 18 points on building roofs. Seven geomatics engineering major graduate students without intensive stereoscopic training are involved as operators in the study. The test organizer requests that all operators measure the 36 feature points at two resolutions (25- μ m and 50- μ m pixel sizes) by using Auto3D toolkit and common photogrammetric workstation. During the measurement, the operators should follow the measuring specification prepared by the test organizer. In the specification, the exact location of each feature point is verbally described and illustrated with an image clip of 150x150 pixels. Figure 7 presents two of the feature points selected for measurement in the tests.



Figure 7. Examples of selected feature points for measurement (left: ground; right: roof)

For comparison purpose, a popular digital photogrammetric workstation is also used to conduct the same measurement. The software supporting the stereoscopic measurement on Windows system is Socet Set. The workstation equips with a regular 19" CRT monitor and requires operators wearing shutter glasses,

which is NuVision 60GX stereoscopic wireless LC glasses produced by MacNaughton, Inc. The alternating field rate of this wireless LC glasses is 120 Hz (60 Hz per view). Under this field rate, the left image and right images are alternately displayed at one instant for each corresponding eye. During the display interval, the LC-shutter blocks out each view by providing time-multiplexing binocular parallax. For synchronization, an infrared emitter is connected to the computer that is operated for the left and right images from a pair of stereo. This emitter generates a synchronization signal that is decoded by the eyewear for accurately switching the LC-shutters. In addition, a 3-pin connector into a compatible graphic card and the eyewear is automatically activated whenever a stereo application is running. The refresh display rate of the graphic card can be accommodated to the most 120 Hz. While 120 Hz is the optimal rate, lower refresh rates are entirely acceptable in order to accommodate a much wider variety of display options. For our tests, we adjusted the display resolution to 1024x768 and the refresh rate to 75 Hz.

To provide independent ground truth without potential side effect of stereoscopic and autostereoscopic measurement, reference measurement is prepared by the test organizer, who uses Adobe Photoshop 5.0 to measure left and right images coordinates of the selected features.

The study is primarily to evaluate the consistency of the autostereoscopic measurements and comparing them with the results from stereoscopic and monoscopic measurements.

5.2 Consistency of autostereoscopic measurements

This section will evaluate the consistency of autostereoscopic measurements from different operators. Since seven operators measure all the 36 feature points, the standard deviation can be calculated respectively for x-left, x-right and y coordinates at each feature points. Therefore, in total there are 3x36 standard deviations calculated, respectively for the 25 μ m and 50 μ m resolution images. Their distributions are plotted in Figure 8. This figures indicate that the majority (> 85%) of the inconsistency among operators is less than 2 pixels. About 15% are within the range of 2-3 pixels. It should be noted that the consistency of measurements tends to be dependent on the image resolution. The lower the image resolution, the more consistent (small standard deviation) the measurements in terms of pixel size. This possibly suggests the resolution limitation of the autostereoscopic monitor.

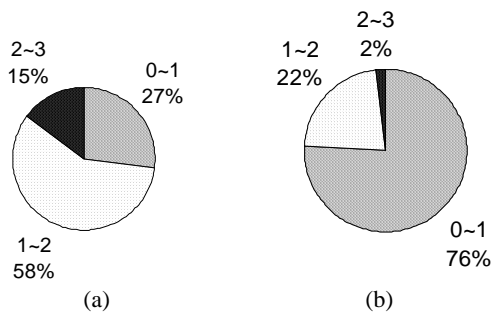


Figure 8. Distribution of standard deviations in pixels among operators (a) 25 μ m. (b) 50 μ m.

5.3 Comparison with other measurements

The autostereoscopic measurements are compared with stereoscopic and monoscopic ones. The type of test discussed here is the paired t test. For the comparison of the differences between two observations by using the autostereoscopic, stereoscopic and monoscopic measurement, the paired t test is evaluated according

$$H_o: \mu_{diff} = 0, H_a: \mu_{diff} \neq 0, t = \frac{\bar{X}_{diff}}{S_{diff} / \sqrt{n}} \quad (6)$$

under the condition of rejecting H_0 if $|t| \geq t_{\alpha/2, (n-1)}$, where μ_{diff} denotes the mean population difference, \bar{X}_{diff} is the sample mean difference, S_{diff} represents the sample standard deviation of the difference, and n is number of points.

In the paired t -test, we compare every point measured for both autostereoscopic (Auto3D) and stereoscopic (Socet Set) systems to the point of reference measurement (Photoshop). Moreover, every point measured with the autostereoscopic system is also compared to the point from the stereoscopic system. Such statistics are evaluated for the x -coordinate measurements on both left and right image, respectively. Note that since the images are epipolar normalized initially, the values of y -coordinate for each feature point are specified as the same. We calculate the differences between coordinate values of the points measured by using different types of systems for every identical feature point. A 95% confidence interval is applied for mean difference here. If the confidence interval for the combination contains zero and the p -value is greater than 0.05, then the points are not statistically different. Our statistical results are presented in Table 1 for the resolutions of 25- μ m and 50- μ m pixel size, respectively.

A few analyses can be made on Table 1. The statistic exhibits significant differences between autostereoscopic and stereoscopic measurements for x -left observations under the resolution of 25 μ m and 50 μ m pixel size. The measurement for 50 μ m x right observation has difference between autostereoscopic and stereoscopic systems. Notice that for y observation the difference between autostereoscopic and stereoscopic measurement shows significant difference under the resolution of both 25 μ m and 50 μ m pixel sizes. The statistic significant differences derived from the measurements for the autostereoscopic system are generally larger than stereoscopic and monoscopic measurements. Moreover, the results indicate that under the resolution of 25 μ m pixel size, the differences of the autostereoscopic measurement are larger than that of stereoscopic measurement for both x -left and y -observations. In contrast, under the resolution of 50 μ m pixel size all results obtained by using the autostereoscopic system are larger than those from stereoscopic system. However, the maximum differences between autostereoscopic and stereoscopic systems in x coordinates for left image are 3.6 and 2.1 pixels under the resolution of 25 μ m and 50 μ m pixel sizes, respectively. The corresponding maximum differences in y coordinates are 1.6 and 1.3 pixels. The maximum difference of either the x -coordinate measurements for left and right image or the y -coordinate measurements is less than 4 pixels under the resolution of 25 μ m and 50 μ m pixel sizes.

Table 1. Statistics of paired t-test in pixels [probability (p-value)/(min difference, max difference)]

	Auto3D-Socet Set	Auto3D-Photoshop	Socet Set - Photoshop
x-left (25 μm)	3.39E-05 (-0.735, 3.623)	0.002 (-1.282, 2.931)	0.177 (-3, 2.952)
x-right (25 μm)	0.895 (-1.565, 1.308)	0.242 (-2.762, 1.971)	0.233 (-0.667, 2.333)
y (25 μm)	0.001 (-1.657, 1.632)	0.709 (-1.943, 1.429)	0.004 (-2, 1.667)
x-left (50 μm)	4.52E-10 (-0.738, 2.149)	0.033 (-1.750, 1.503)	0.001 (-2.524, 1.096)
x-right (50 μm)	0.008 (-1.085, 1.129)	0.063 (-1.553, 1.443)	0.661 (-1.904, 1.096)
y (50 μm)	3.79E-05 (-0.654, 1.273)	0.086 (-0.935, 1.411)	0.083 (-1.238, 1.286)

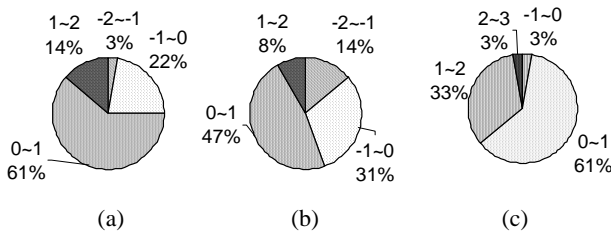


Figure 9. Distribution of differences (Auto3D-Socet Set) in pixels (25 μ m images). (a) x-left. (b) x-right. (c) y.

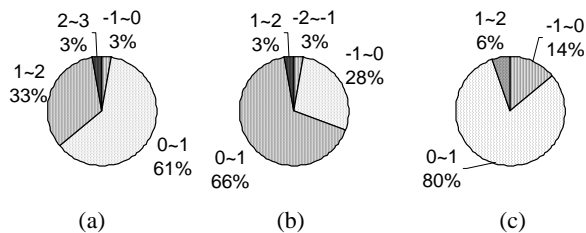


Figure 10. Distribution of difference (Auto3D-Socet Set) in pixels (50 μ m images). (a) x-left. (b) x-right. (c) y.

This range not only suggests not much significant difference in practical of autostereoscopic and stereoscopic observations, but also indicates the approximately close maximum errors on point identification between these two systems. The results demonstrate that the autostereoscope can be a reliable measurement system in contrast with the traditional eyeglasses-based systems, especially for handling a large volume of data with limited resources and with the expectation of no significant loss in photogrammetric accuracy. Finally, notice that the 3D perception among all the seven participant observers slightly degrades because some points are difficult to be digitized as a consequence of the lower color contrast or ambiguous definition and interpretation on their precise locations. Nevertheless, our measurement errors are consistent and follow the same or very similar distribution.

6. CONCLUSION

In this paper, we investigate the potential and performance of autostereoscopic measurement as a possible technical alternative in photogrammetric practice. For this objective, we first analyze the general 3D geometry of an autostereoscopic system. The analyses are devoted to the parameters of viewing zone, including its geometric shape, corresponding size, and the

movement boundary of operators for photogrammetric practice. Because the movement boundaries are addressed within the optimum viewing zones for operators during photogrammetric practices, we also estimate the perceived depth that directly affects the accuracy of the autostereoscopic measurement. The analysis indicates that longer perceived depth provides observer a sharper 3D sense. Furthermore, to demonstrate the performance of autostereoscopic measurement, we implement several photogrammetric tests to compare both the stereoscopic and autostereoscopic measurement with a standard measurement. We first introduce the measuring systems and our software, Auto3D, designed for DTI 3D monitor based on the parallax-barrier system. Finally we present statistical analyses for comparison. Our results show that over all more than 62% of the autostereoscopic measurements are less than one pixel away from the popular stereoscopic measurements. The consistency of autostereoscopic measurements from different operators is better than 1 pixel for at least 60% of the measurements.

7. REFERENCES

- Hattori, T. (1991). Electro optical autostereoscopic displays using large cylindrical lenses, SPIE Proceedings, Stereoscopic Displays and Applications II, Editors, John O. Merritt, Scott S. Fisher, Vol. 1457, 283-289, February, 25-27, San Jose, California.
- Jones, G., Lee, D., Holliman, N. and Ezra, D. (2001) Controlling perceived depth in stereoscopic images, Proceedings of SPIE, Vol. 4297 Stereoscopic Displays and Virtual Reality Systems VIII.
- Motoki, T., Isono, H. and Yuyama, I. (1995) Present Status of Three-Dimensional Television Research, *Proceedings of IEEE*, Vol. 83, pp. 1009-1021.
- Okoshi, T. (1976) Three Dimensional Imaging Techniques, Academic, New York.
- Okoshi, T. (1980) Three Dimensional Displays. Proc. IEEE Vol. 68, pp. 548-64.
- Pastoor, S. and Wöpking, M. (1997) 3D Displays: A review of current technologies, Displays Vol. 17, pp. 100-110.
- Petrie, G. (2001). 3D Stereo-Viewing of Digital Imagery: Is Auto-Stereoscopy the Future for 3D?, *GeoInformatics*, Vol. 4, No. 10, 24-29.
- Sexton, I. (1992) Parallax Barrier Display Systems, In IEE Colloquium on Stereoscopic Television, volume Digest 173, pp 5/1-5/5.
- Shan, J. Fu, C. Li, B. Bethel, J., Kretsch, J. And Mikhail. E. (2004) Autostereoscopic measurement: principles and implementation, ASPRS Annual Conference, Denver, Colorado.
- Son, J. Y., Saveljev, V. V., Choi, Y. J., Bahn, J. E., Kim, S. K. and Choi, H. (2003) Parameters for designing autostereoscopic imaging systems based on lenticular, parallax barrier, and integral photography plates, *Opt. Eng.* Vol. 42, pp. 3326-3333.

ACKNOWLEDGEMENT

This work is sponsored by the National Geospatial-Intelligence Agency.